Study of charge sharing effect and energy resolution of the Timepix hybrid detector based on gallium arsenide compensated with chromium

Lisan David Cabrera Gonzalez[1], Antonio Leyva Fabelo[2,3], Petr Smolyanskiy[4], Alexey Zhemchugov[3], Ernesto Alfonso Pita[4], Annie Meneses González[2]

[1] University of Pinar del Rio (UPR)
[2] Center for Technological Applications and Nuclear Development (CEADEN)
[3] Joint Institute for Nuclear Research (JINR)
[4] Higher Institute of Technology and Applied Sciences (InsTEC)

lisan.cabrera@upr.edu.cu; lisandcabrera@gmail.com

Abstract

Among the latest ionizing radiation detectors, those based on chromium compensated gallium arsenide (GaAs:Cr) are ones of the most competitive for many applications due to their high Z and strong resistance to radiation damage. They have been used in high energy physics research, medical visualization and spatial technologies, geological prospecting, among other advanced fields. The object of this work is a 900 μm GaAs:Cr detector with Timepix readout technology. Some detector characteristics for three experimental conditions were measured and studied by using the X-rays from a synchrotron and an X-ray tube provided with different materials for obtaining the corresponding fluorescence photons. A complex function was used to decompose the differential spectra into the most important contributions involved. As an additional tool for the research, the mathematical modeling of the mobility of charge carriers generated by radiation within the active volume of the detector was used. The results of these charge sharing effect studies showed a noticeable prevalence in the detector of this effect, changing its contribution according to the experiment characteristics. The detector was calibrated for the planned experiments and the energy resolution was determined. From the analysis of all the obtained results and their comparison with those reported in literature, it was confirmed that the detector has a marked charge-sharing effect between neighboring pixels, being its performance more impaired as the energy of incident photons increases.

Key words: energy resolution; experimental data; calibration; energy spectra; radiation detectors; high energy physics; charge distribution.

Estudio del efecto de compartición de cargas y la resolución energética del detector híbrido Timepix de arseniuro de galio compensado con cromo

Resumen

Entre los últimos detectores de radiación ionizante, los basados en arseniuro de galio compensado con cromo (GaAs: Cr) son de los más competitivos para muchas aplicaciones debido a su alto Z y fuerte resistencia al daño de la radiación. Se han utilizado en investigación de física de alta energía, visualización médica y tecnologías espaciales, prospección geológica, entre otros campos avanzados. El objeto de este trabajo es un detector de GaAs: Cr de 900 μm con tecnología de lectura Timepix. Algunas características del detector para tres condiciones experimentales se midieron y estudiaron utilizando rayos X de un sincrotrón y un tubo de rayos X provisto de diferentes materiales para obtener los fotones de fluorescencia correspondientes. Se utilizó una función compleja para descomponer los espectros diferenciales en las contribuciones más importantes involucradas. Como herramienta adicional para la investigación, se utilizó el modelado matemático de la movilidad de los portadores de carga generados por la radiación dentro del volumen activo del detector. Los resultados de estos estudios de efecto de carga compartida mostraron una prevalencia notable en el detector de este efecto, cambiando su contribución según las características del experimento. El detector se calibró para los experimentos planificados y se determinó la resolución de energía. A partir del análisis de todos los resultados obtenidos y su comparación con los reportados en la literatura, se confirmó que

el detector tiene un marcado efecto de reparto de carga entre píxeles vecinos, y su rendimiento se ve más afectado a medida que aumenta la energía de los fotones incidentes..

Palabras clave: resolución en energía; datos experimentales; calibración; espectros de energía; detectores de radiaciones; física de altas energías; distribución de cargas.

Introduction

The collaboration between the State University of Tomsk and the JINR has some important successes in applications of hybrid pixelated detectors with GaAs:Cr as sensor material, connected to an advanced readout electronic known as Timepix [1]. An example of this is a MARS microtomograph [2], which is used for many purposes, as biomedical researches and geophysical studies.

Although certain results have been obtained, it is desirable to reach a deeper knowledge of the characteristics and properties of the pixelated detector provided with GaAs:Cr to develop and further diversify its applications.

A very important aspect to pay attention is the phenomenon of the charge sharing between neighboring pixels [3], which affects the resolution and efficiency of the device, as well as other properties. This phenomenon is related to the charges movement directed to a target pixel inside the biased detector active volume, inducing charge do not only in this pixel, but also in its neighboring pixels.

Many factors contribute to this effect, such as the incoming radiation direction, the pixels dimensions, the separation between them, the electrons cloud dimensions, the applied polarization potential and the material diffusion coefficient.

Due to the importance of the charge sharing contribution to the detector performance, that its study is a research priority within the segmented detectors.

The present work is dedicated first to study some peculiarities of this phenomenon in a detector in study, using mathematical modeling and the differential pulse height spectrum. And secondly, the device energy calibration was performed for two experimental conditions and the device energetic resolution was determined.

Materials and methods

Modeling methods

For the mathematical modeling of the beam sweep the initial cloud center was placed 15 μm next to the cathode inside the active material, most likely position for low energy photons verified in previous simulations with the MCNPX code system [4] reported in [5,6]. The cloud diameter (2.5 μm) was established based on the calculation of the generated photoelectrons range [7]. The sensor anode is segmented forming a 256 x 256 matrix, with 45 x 45 μm^2 pixels and 10 μm gap.

The cloud induced charge on the target pixels(Q) is a detector characteristic that leads to the magnitu-

de influence of the charge sharing effect in the detector response. In order to obtain the induced by the carriers cloud charge during its drift and diffusion movement was used the Shockley-Ramo theorem [3] (eq.1)

$$Q=q\Delta\varphi_0, \qquad \text{eq.1}$$

where q is the punctual carrier charge value and $\Delta\varphi_0$ is the weighting potential difference at the initial cloud position and at the detector anode location, value obtained with the employment of the ARCHIMEDES 2.0.1code system [8].

Experimental setup and methods

As radiation sources were employed the X-rays generated by a VEPP-3 synchrotron of the Budker Institute of Nuclear Physics [9], and by an X-ray tube with different materials for obtaining the corresponding fluorescence photons (table 1) provided by the Dzheliepov Laboratory of Nuclear Problems (DLNP) of the JINR.

Table 1. Experimental and calculated $T_{1/2}$ for ^{98}Cd and ^{98}Ag

Sources -->	Fluorescent X–rays	Synchrotron	
Cases -->	Pixelarrangement	1 pixel	Gap between two adjacent pixels
Energy (keV) -->	15.691 (Zr)	12	18
	17.375 (Mo)	18	
	20.074 (Rh)	27.9	
	22.964 (Cd)	40	
	25.044 (Sn)		

The fine collimated synchrotron beam was used to irradiate point zones of independent pixels, as well as to perform the line sweep between two continuous pixels. The X-ray tube with a reflection configuration allowed to irradiate larger areas including several pixels at the same time.

This detector presents fourth possible operation modes, but is only used the "Single photon" mode for convenience. This approach delivers the number of times that signal exceeds the threshold level (THL) while the shutter is still open. This number of times by THLis the relation experimentally known as the integral pulse height spectrum [3].

The method employed [10] to experimentally study the charge sharing effect and obtain the detector energy resolution consists in fitting the observed points of the integral pulse height spectrum to a general function F(x). Then gets the correspondent differential pulse height spectrum f(x) and the different sub functions that com-

pound it, each one describing a particular effect to take into account.

The function that describe the charge sharing effect is one from a function family called "repetitive integrals of the complementary error function" [11], numerically calculated by:

$$i^a Erfc(x) = \sum_{j=0}^{\infty} \frac{(-1)^j x^j}{2^{a-j} \cdot j! \cdot \Gamma\left(1 + \frac{1}{2}(a-j)\right)}, \quad \text{eq. 2}$$

where Γ is the Gamma function, j the iterative variable, a the integration order and $i^a Erfc$ is the order a complementary error function integral. Was concluded that the order 2 complementary error function integral is the adequate function to describe the charge sharing effect contribution.

Other of these sub functions is the known "complementary error function" [12]:

$$Erfc(x) = \frac{2}{\sqrt{\pi}} \int_x^{\infty} e^{-u^2} du, \quad \text{eq. 3}$$

where u is the integration variable. $Erfc(x)$ describe appropriately the counts behavior without considering the charge sharing effect corresponding function. Finally, a linear function is considered, which slope d is the background counts, and a constant g with fitting purposes only.

The applied general function to fit the experimental points is then:

$$F(x) = b \cdot i^2 Erfc\left(\frac{x-\mu}{\sqrt{2} \cdot \sigma}\right) +$$
$$c \cdot \frac{1}{2\sqrt{2} \cdot \sigma} Erfc\left(\frac{x-\mu}{\sqrt{2} \cdot \sigma}\right) + d \cdot \left(\frac{x-\mu}{\sqrt{2} \cdot \sigma}\right) + g, \quad \text{eq. 4}$$

Where b is the charge sharing effect contribution corresponding parameter, c the energy peak corresponding parameter, μ the THL mean value and the corresponding standard deviation.

Once fitted the function, is only needed derive F(x) to get the differential pulse height spectrum f(x):

$$f(x) = b \cdot i^1 Erfc\left(\frac{x-\mu}{\sqrt{2} \cdot \sigma}\right) + c \cdot \frac{1}{\sqrt{2\pi} \cdot \sigma} e^{-\left(\frac{x-\mu}{\sqrt{2} \cdot \sigma}\right)^2} + d, \quad \text{Eq. 5}$$

This is the standard procedure applied to three cases, chosen under the base that charge sharing effect is manifested differently in each one, such cases are:

1. The radiation is directed to an arrangement of pixels.
2. The collimated beam is directed to the center of a pixel.
3. The collimated beam is directed to the gap between two adjacent pixels.

After been obtained the corresponding μ and σ parameters, is performed the calibration curve. Then the energy resolution is found to be [3]:

$$R = \frac{FWHM}{E_x}, \quad \text{Eq. 6}$$

where R is the energy resolution, FWHM is the full width at half maximum ($\approx 2.35\sigma$) and Ex is the peak energy.

Modeling results and discussion

Figure 1 presents the induced charge modeling during the beam sweep from a pixel center to the center of the next one. The secondary electron cloud diameter and the interaction position inside the detector active volume are relevant elements to analyze in order to study the induced charge and the charge sharing effect in sensitive pixels.

The electron cloud diameter influence and the interaction position contribution to the simulated induced charge are shown in the figure 1 (a) and figure 1 (b) respectively. The figure 1 (a) simulated initial clouds are positioned at a constant initial distance of 885 μm between their center and the detector anode surface. The interaction positions shown in figure 1 (b) are represented by the distance between the interaction position and the anode surface.

The behavior found in the mathematical modeling is similar to the modeling presented in [13] and the expe-
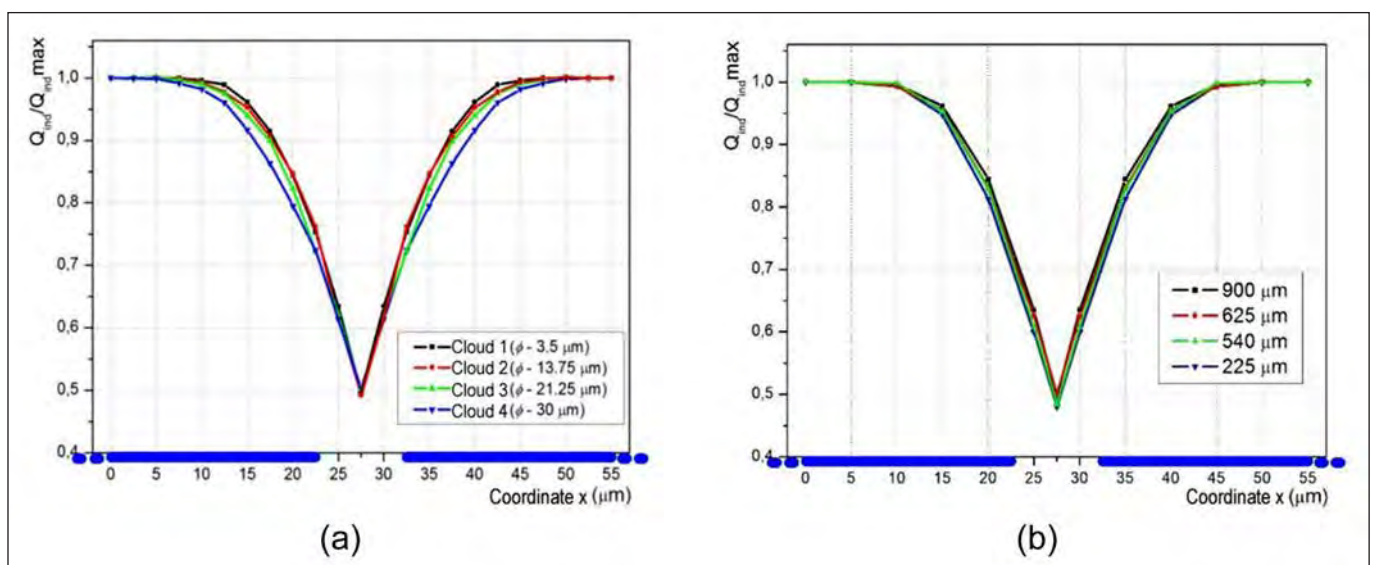

Figure 1. Mathematical modeling of the normalized induced charge in two neighboring pixels during the beam sweep along the initial generated electrons cloud position at the x axis for four electron cloud diameters (a) and for four interaction deeps (b).

rimental results seen in [14]. In both cases, although the detector material is different (Si and CdZnTe respectively), a behavior characterized by a plateau on the pixels central zone is verified, and a fall that extends to the gap center, where the signal intensity decreases to 45 - 50% of the recorded maximum. These two articles and other similar results such as [15] confirms the adequate correspondence of the used model with the already performed experiments.

The results presented in figure 1 (a) shows that dependence between the cloud sizes of charge carriers generated at the time of the interaction of the photons with the GaAs:Cr does not significantly influence the induced charge values in the pixels, as long as the number of generated charges remains constant (103 electrons).

On the other hand, in the figure 1 (b) is verified that, within the studied limits, the depth at which the photon interaction occurs is not significant to the induced charge in the pixels. This is a direct consequence of the well-known "small pixel effect" [3]. At a distance lower than 100 μm for this 900 μm detector, a strong influence on the results is expected, since it is the area where the weighting potential starts its abrupt growth [6].

Experimental results and discussion

An example of the applied full procedure to get the detector energy resolution and study the charge sha-

ring effect contribution in the integral and differential pulse height spectrum is presented in the next figure, for the irradiation to a 230x230 pixels arrangement with 15,691 keV X rays. The differential pulse height spectrum of figure 2 (c) represents functions that characterizes the total counts (red), the charge sharing effect (green), the energy peak gauss distribution (blue) and the background (black).

For free fitting parameters are consider μ, σ, b, c, d and g. figure 2 (c) and (d) y axis values are different because in the first one is shown the derivative of F(x) respect to $\frac{x-\mu}{\sqrt{2}\cdot\sigma}$, while in the second one is represented the derivative with respect to x of the experimental points shown in figure 2 (a).

The gauss distribution parameters (μ,σ) are used to find the detector energy resolution for the incoming X rays energies considered in table 1. Mean while the charge sharing effect contribution function is used to study this effect, through comparison with the remaining two cases.

The same procedure is applied to the collimated beam directed to a pixel center case with 27,9 incoming keV X rays (figure 3) and the collimated beam directed to the center of the gap between two neighboring pixels case with 18 keV incoming X rays (figure 4).
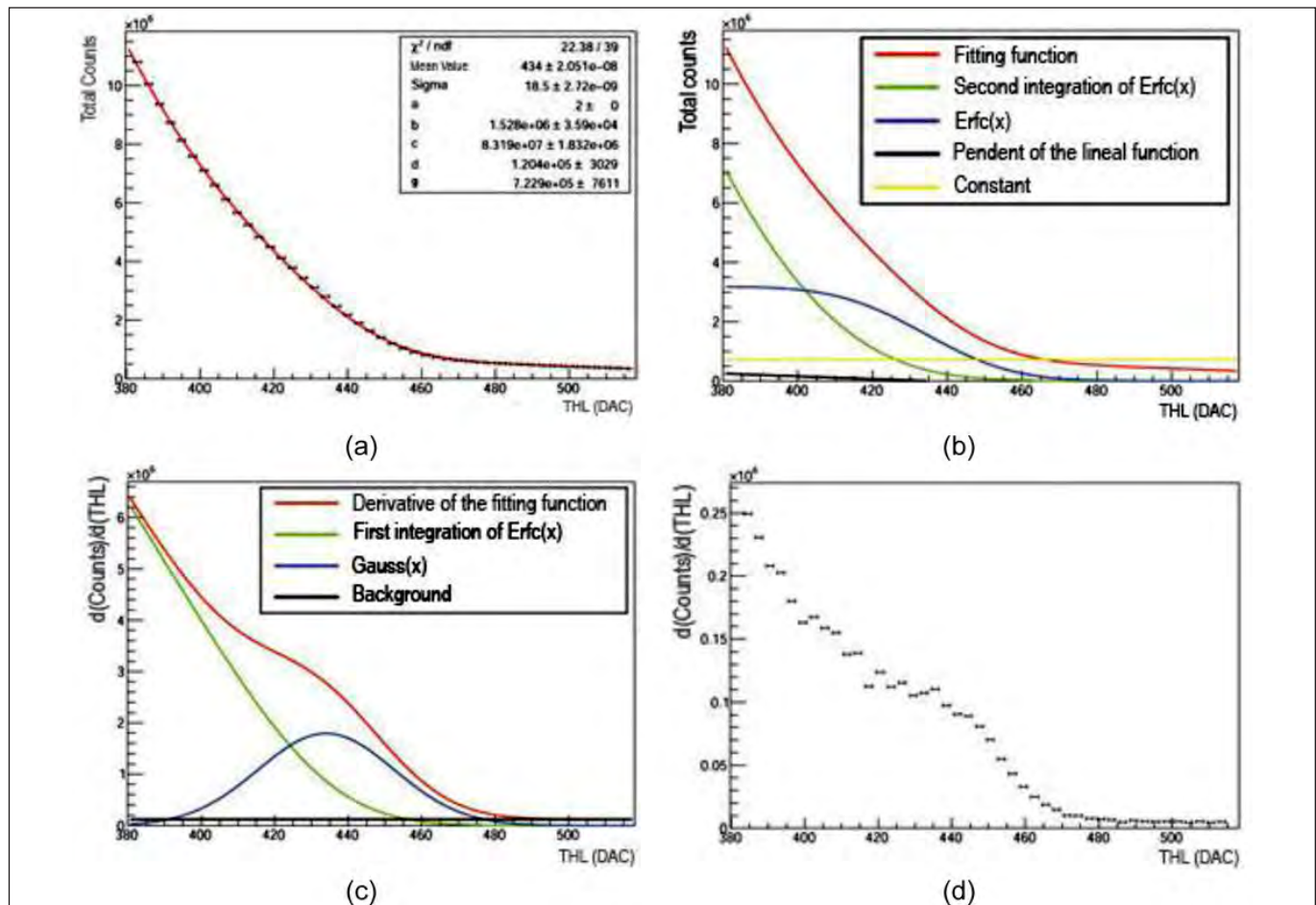

Figure 2. Pixel arrangement irradiation experimental spectrum procedure; (a) counts vs. THL experimental dependence with their corresponding F(x) fitting function, (b) fitting function decomposition in its components, (c) derivative fitting function with its components, (d) derivative experimental points.
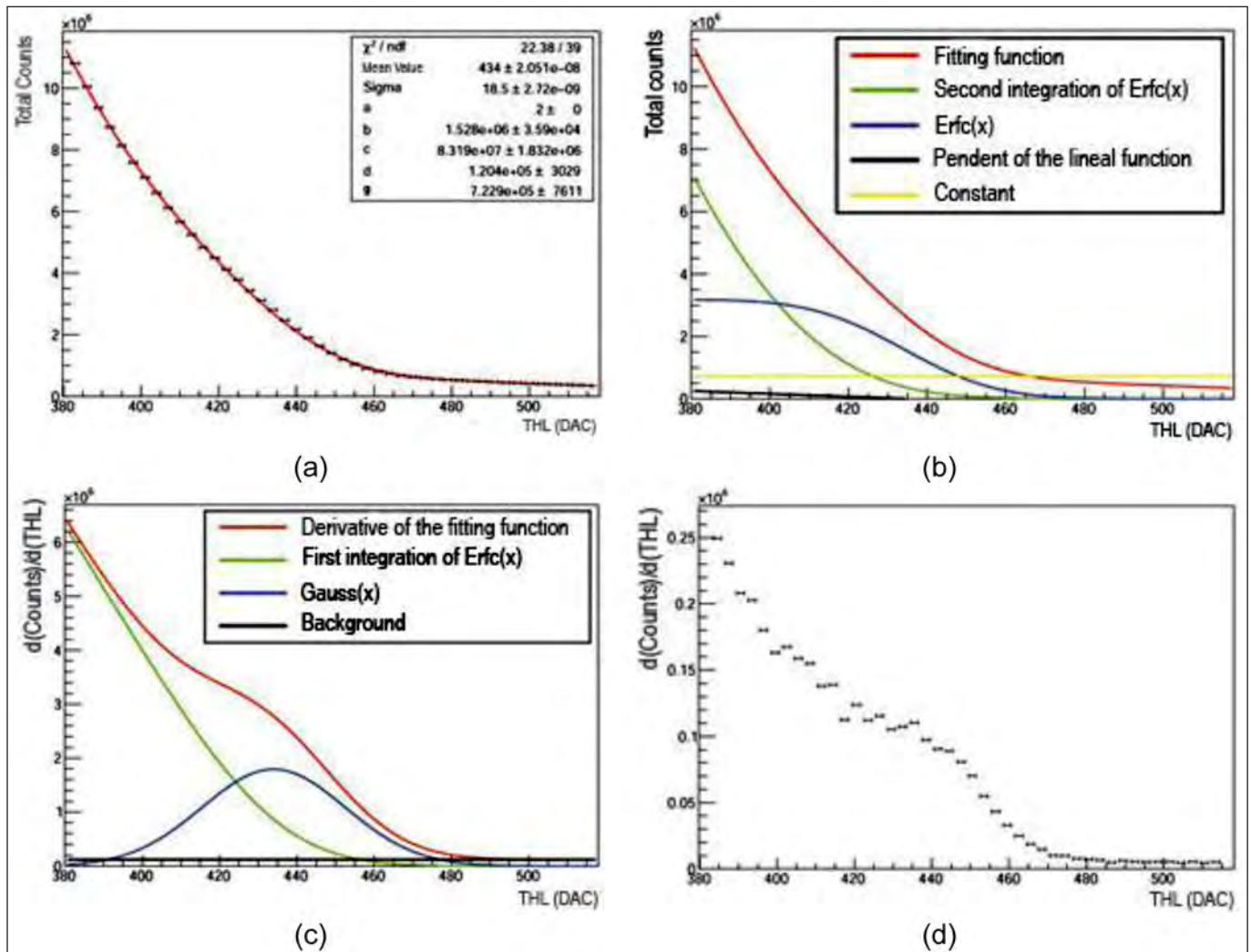
Figure 3. Pixel arrangement irradiation experimental spectrum procedure; (a) counts vs. THL experimental dependence with their corresponding F(x) fitting function, (b) fitting function decomposition in its components, (c) derivative fitting function with its components, (d) derivative experimental points.

For both neighboring pixels, the gap irradiation case procedure, showed through figure 4, presents the counts vs. THL experimental dependence with their corresponding F(x) fitting function (figure 4 (a) and (c) respectively), and the derivative fitting function with its components (figure 4 (b) and (d) respectively).

In order to compare the charge sharing effect contributions for the several analyzed configurations is defined the quotient η:

$$\eta = \frac{b}{c}$$ Eq. 7

The attenuation of the energy peak gauss distribution by the charge sharing effect is exposed with the coefficient η. A comparison between the observed cases is presented in table 2.

The higher charge sharing effect contribution is presented in the pixel arrangement irradiation case, followed by the irradiation directed to gap between two neighboring pixels case, and finally the irradiation directed to a pixel center, facts verified by figures. 2, 3, 4 and table 2.

The charge sharing effect contribution depends on the irradiation beam transversal section, its target zone, and others factors mentioned previously. This effect

contribution is larger as larger the beam transversal section is and involved pixels are. The induced charge registered in the gap irradiation case is lower than the corresponding incoming radiation energy reported [16], reason why is excluded this case in following analysis.

Table 2. η value for each case

Cases	Pixelarrangement	1 pixel	Gap between two adjacent pixels
η	0.018367±0.000836	0.001753±0.000022	0.004163±0.000006 0.003906±0.000224

This detector calibration, for the pixel arrangement irradiation case and the irradiation directed to a pixel center case, seen in figure 5 (a), is defined as the ratio between the incoming X rays energies and their corresponding THL peak value, this last one assigned by the analog-digital converser (DAC) [9].

Once developed the detector calibration is used Eq. 6 to obtain the detector energy resolution, presented in figure 5 (b).

Each pixel possesses its own electronics and therefore its own electronic noise, which means that each pixel has its own THL different from the others [17], this
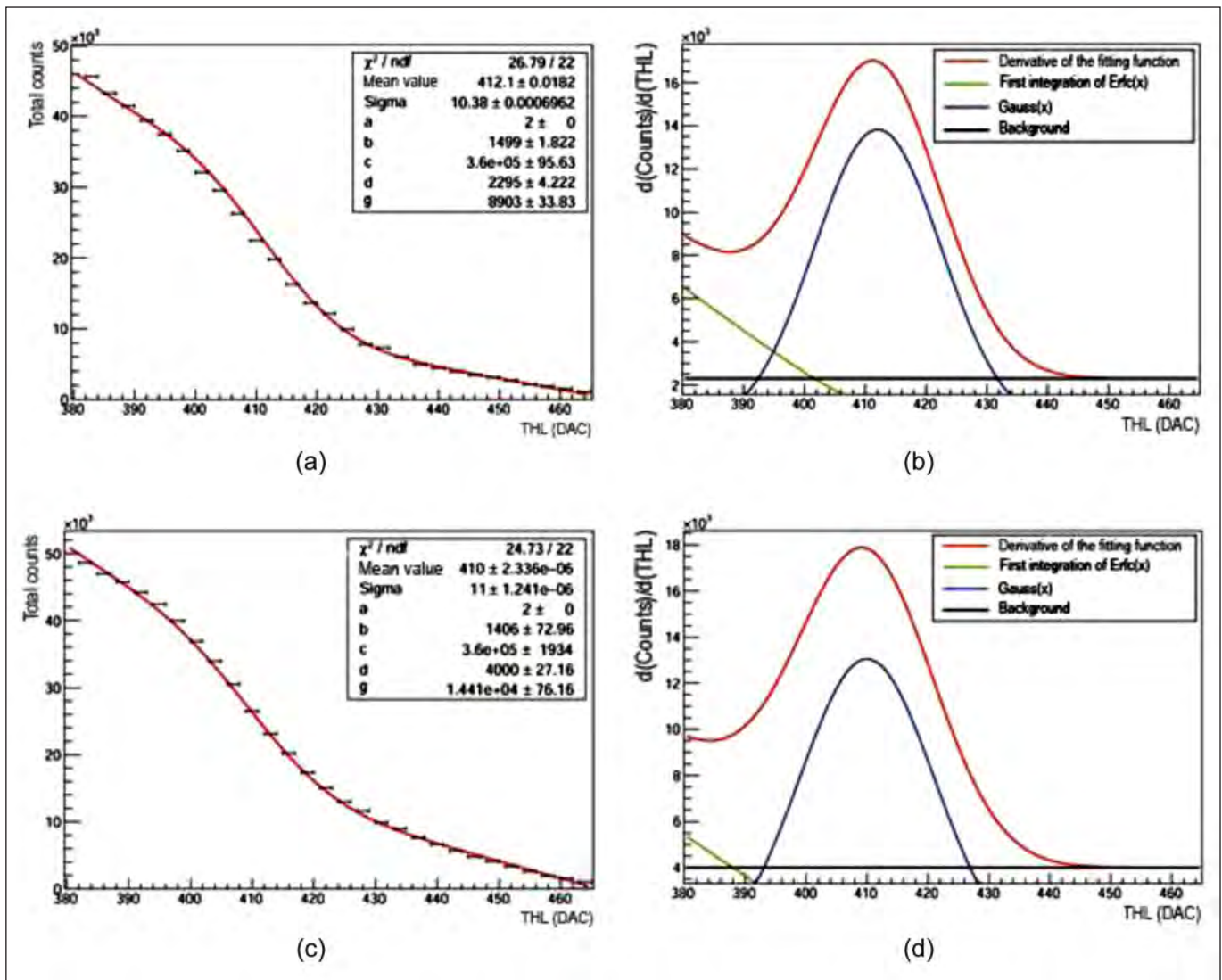
Figure 4. Irradiation directed to the gap center experimental spectrum procedure.
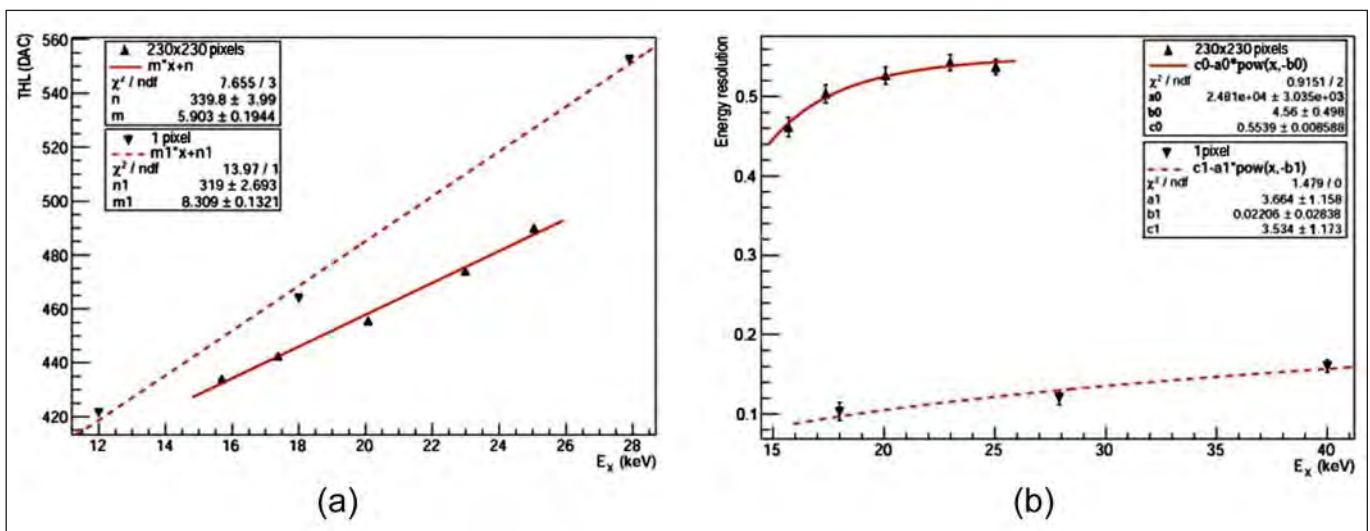

Figure 5. Calibration curve (a) and energy resolution (b) for discussed cases

is reflected in the calibration curve by the two different linear fitting functions shown in figure 5 (a).

Figure 5 (b) reveals that energy resolution is improved for lower incoming X rays energies values in both cases, and affected negatively by the charge sharing effect, whose contribution is greater as bigger the collimated beam transversal section is.

Conclusion

The mathematical modeling of the charge collection process is verified by the experimental analysis and reached results, confirmed by the observation that in the irradiated middle gap point between adjacent pixels the detected induced charge is lower, and the charge sharing effect is bigger. The selection of the initial cloud dimensions of generated charges, and their distance to the surface where the anodes are located, are not critical aspects for the mathematical modeling results within the studied limits.

Was possible, using a standard procedure and a general function, to get more precisely the differential pulse height spectrum and the several involved effects contributions, for their comparison and understanding. It was studied three cases, depending to the way that pixels were irradiated, concluding that charge sharing effect contribution is higher when a pixel arrangement is irradiated, than when a single pixel is.

This phenomenon is reflected in the detector energy resolution, which is better, within the studied limits, for lower incoming energies, for smaller collimated beam transversal sections and for center focused collimated beams.

It was verified using the analysis and comparison with the literature, that this detector presents a marked charge sharing effect between pixels, phenomenon that negatively influence its performance when the incoming photons energies increase.

Acknowledgement

Bibliographic References

[1] MEDIPIX. 2011. Available in: http://medipix.web.cern.ch/medipix/ [consulting date: may 8, 2016].

[2] POTRAP I, KOZHEVNIKOV D. Spectral microtomography using the MARS-CT. 2013. Available in: http://newuc.jinr.ru/img_sections/file/project/2014/MarsProject.pdf [consulting date: may 24, 2016].

[3] KNOLL GF. Radiation detection and measurement. Michigan: John Wiley & Sons, Inc., 2000. Third Edition. ISBN: 978-0-470-13148-0.

[4] BRIESMEISTER JF. MCNP - a general Monte Carlo n-particle transport code. LA-13709-M. 2000. version 4C. Los Ángeles.

[5] MENESES A. Estudio mediante el método de Monte Carlo del transporte de fotones y del proceso de colección de cargas en detectores híbridos pixelados de GaAs:Cr. [bachelor thesis]. Higher Institute of Technology and Applied Sciences. Havana, 2015.

[6] MENESES A, LEYVA A, PINEIRA I, CRUZ CM, et. al. Spatial distribution of X and gamma rays induced energy deposition on semi-insulating GaAs:Cr based pixel radiation detector. Proceedings of X Workshop on Nuclear Physics and IX International Symposium on Nuclear and Related Techniques. 2015. vol. 654, no. 5, p. 208-212. ISBN: 978-959-300-069-7.

[7] NIST. 2015. Available in: http://physics.nist.gov/PhysRefData/Star/Text/ESTAR.html [consulting date: may 23, 2016].

[8] SELLIER JMD, FONSECA JE, KLIMECK G. Archimedes, the free Monte Carlo simulator. Proceedings of the 15th International Workshop on Computational Electronics. doi: 10.1109/IWCE.2012.

[9] BUDKER INSTITUTE OF NUCLEAR PHYSICS. The VEPP-3 electron-positron storage ring. 2016. Available in: http://v4.inp.nsk.su/vepp3/index.en.html [consulting date: jun, 5 2016].

[10] VAN DER BOOG RPM. Energy calibration procedure of a pixel detector. 2013. National Institute for Subatomic Physics [bachelor thesis of applied physics]. https://wiki.nikhef.nl/detector/pub/Main/ArticlesAndTalks/Energy_calibration_procedure.pdf

[11] NIST. 2015. Digital library of mathematical functions. Available in: http://dlmf.nist.gov/7.18 [consulting date: may 14, 2016].

[12] WEISSTEIN EW. Erfc. 2016. Available in: http://mathworld.wolfram.com/Erfc.html [consulting date: may 14, 2016].

[13] ARFAOUI S. Calibration, simulation and test-beam characterization of Timepix hybrid-pixel readout assemblies with ultra-thin sensors. International Workshop on Future Linear Collider. The University of Tokyo. 11-15 November 2013. CERN/PH-LCD.

[14] MCCONNELL M, MACRI JR, RYAN JM. Three-dimensional imaging performance of orthogonal coplanar CZT strip detector. SPIE's 45-th Annual Meeting. San Diego, 2000.

[15] BOLOTNIKOV AE, COOK WR, HARRISON FA. Charge loss between contacts of CdZnTe pixel detectors. NIM A. 1999; 432(7): 326-331. PII: S0168-9 002 (99)003 88-5.

[16] BRÖNNIMANN C, FLORIN S, LINDNER M, et. al. Synchrotron beam test with a photon-counting pixel detector. J. Synchrotron Rad. 2000; 429(7): 301-306.

[17] BUTLER AP, BUTLER PH, BELL ST, et. al. Measurement of the energy resolution and calibration of hybrid pixel detectors with GaAs:Cr sensor and Timepix readout chip. NIM A. 2015; 457(2): 234-256. doi: 10.1134/S1547477115010021.